Journal of Inorganic Biochemistry 172 (2017) 138–146

Contents lists available at ScienceDirect

Journal of Inorganic Biochemistry

journal homepage: www.elsevier.com/locate/jinorgbio

Novel copper(II) complexes with hydrazides and heterocyclic bases: Synthesis, structure and biological studies

Drielly A. Paixão[a], Ivana M. Marzano[b], Edgar H.L. Jaimes[b], Marcos Pivatto[a], Débora L. Campos[c], Fernando R. Pavan[c], Victor M. Deflon[d], Pedro Ivo da S. Maia[e], Ana M. Da Costa Ferreira[f], Isadora A. Uehara[g], Marcelo J.B. Silva[g], Françoise V. Botelho[h], Elene C. Pereira-Maia[b], Silvana Guilardi[a], Wendell Guerra[a,*]

[a] Instituto de Química, Universidade Federal de Uberlândia, Uberlândia, MG, Brazil
[b] Departamento de Química, Universidade Federal de Minas Gerais, Belo Horizonte, MG, Brazil
[c] Faculdade de Ciências Farmacêuticas, UNESP - Universidade Estadual Paulista, Campus Araraquara, 14.800-903 Araraquara, SP, Brazil
[d] Instituto de Química de São Carlos, Universidade de São Paulo, São Carlos, SP, Brazil
[e] Instituto de Ciências Naturais, Exatas e Educação, Universidade Federal do Triângulo Mineiro, Uberaba, MG, Brazil
[f] Instituto de Química, Universidade de São Paulo, São Paulo, SP, Brazil
[g] Instituto de Ciências Biomédicas, Universidade Federal de Uberlândia, Uberlândia, MG, Brazil
[h] Instituto de Genética e Bioquímica, Universidade Federal de Uberlândia, Uberlândia, MG, Brazil

ARTICLE INFO

Keywords:
Copper(II) complexes
Hydrazide
DNA binding
Apoptosis
Antitumoral activity
Mycobacterium tuberculosis

ABSTRACT

Five new copper(II) complexes of the type $[Cu(N{-}O)(N{-}N)(ClO_4)_2]$, in which N−O = 4-fluorophenoxyacetic acid hydrazide (4-FH) or 4-nitrobenzoic hydrazide (4-NH) and N−N = 1,10-phenanthroline (phen), 4–4′-dimethoxy-2-2′-bipyridine (dmb) or 2,2-bipyridine (bipy) were synthesized and characterized using various spectroscopic methods. The X-ray structural analysis of one representative compound indicates that the geometry around the copper ion is distorted octahedron, in which the ion is coordinated to hydrazide *via* the terminal nitrogen and the carbonyl oxygen, and to heterocyclic bases *via* their two nitrogen atoms. Two perchlorate anions occupy the apical positions, completing the coordination sphere. The cytotoxic activity of compounds was investigated in three tumor cell lines (K562, MDA-MB-231 and MCF-7). Concerning K562 cell line, the complexes with 1,10-phenanthroline exhibit high cytotoxic activity and are more active than carboplatin, free ligands and $[Cu(phen)_2]^{2+}$. Considering the cytotoxicity results, further investigations for the compounds $[Cu(4\text{-}FH)(phen)(ClO_4)_2]$ **I** and $[Cu(4\text{-}NH)(phen)(ClO_4)_2]\cdot H_2O$ **III** were performed. Flow cytometric analysis revealed that these complexes induce apoptotic cell death in MDA-MB-231 cell line and bind to DNA with K values of 4.38×10^4 and 2.62×10^4, respectively. These compounds were also evaluated against wild type Mycobacterium tuberculosis (ATCC 27294) and exhibited antimycobacterial activity, displayed MIC values lower than those of the corresponding free ligands.

1. Introduction

Nowadays, there is a great interest in the use of copper complexes in cancer chemotherapy, mainly those containing *N,N*-heterocyclic ligands, such as 1,10-phenanthroline, 2,2′-bipyridine, 2,2′:6′,2″-terpyridine, and derivatives, that facilitate intercalation to DNA. After the report that $[Cu(phen)_2]^+$ complex cleaves DNA, a great number of copper complexes with *N,N*-donors ligands have been synthesized and utilized as artificial nucleases [1]. Moreover, many of these copper compounds have been described to inhibit tumoral cell growth [2–14]. Regarding the clinical utility of these complexes, two of them developed by L. Ruiz and co-workers, are already approved for clinical trials as antitumor drugs [15,16].

Our research group has a great interest in the synthesis and biological evaluation of ternary complexes of copper. As a first example, we reported the DNA cleavage ability of two copper(II)-phenanthroline complexes with tetracycline and doxycycline. Both complexes showed an expressive plasmid DNA cleavage activity, under mild reaction conditions, even in the absence of any additional reducing agent, besides inhibited the growth of a chronic myelogenous leukemia cell line [17]. Furthermore, it was reported that UV-light exposure increases the cytotoxic activities of these copper complexes,

* Corresponding author at: Instituto de Química, Universidade Federal de Uberlândia, João Naves de Ávila Avenue, 2121, Campus Santa Mônica, 38.400-902 Uberlândia, MG, Brazil.
E-mail address: wendell.guerra@ufu.br (W. Guerra).

http://dx.doi.org/10.1016/j.jinorgbio.2017.04.024
Received 21 December 2016; Received in revised form 27 March 2017; Accepted 23 April 2017
Available online 26 April 2017
0162-0134/

which makes them potential agents for photodynamic therapy [18]. In other studies, our research group has also shown that copper(II) complexes containing β-diketones and 2,2′-bipyridine or 1,10-phenanthroline are promising antitumoral agents [19,20]. For example, the compound [Cu(L)(phen)NO_3], in which L = 1-(4-chlorophenyl)-4,4,4-trifluoro-1,3-butanedione, inhibits the growth of K562 cells with an IC_{50} value equal to 2.1 μM [19].

Regarding hydrazides and derivatives, it is known that these compounds exhibit a wide variety of biological activities, including antimycobacterial, antifungal, antibacterial, antioxidant, anti-inflammatory, and antitumoral, among others [21]. This class of compounds has the ability to readily coordinate to many transition metals. Therefore, several hydrazide complexes have been synthesized and characterized [22,23]. Some of these compounds exhibit remarkable biological properties, mainly antimycobacterial and antitumoral [24–32]. For instance, the effect of copper(II) complexes containing hydrazides and *N,N*-heterocyclic ligands on the growth of tumor cells was evaluated by our research group. These complexes were able to enter the cells and inhibit cellular growth in a concentration-dependent manner, with an activity higher than that of the corresponding free ligands [31]. Concerning the pharmacological potential of metal-based drugs, this work was, as much as is from our knowledge, the first to describe anticancer properties of copper(II) complexes with hydrazides and 1,10 phenanthroline or derivatives. In addition, more recently, Bortolotto et al. showed that under UV-light exposure, these complexes enhance the DNA cleavage activity [32]. Indeed, these results show clearly that ternary complexes of copper(II) with hydrazides and heterocyclic bases, such as 1,10-phenanthroline, are very promising as anticancer agents. Aiming to continue this work, we describe herein the synthesis of a new series of complexes containing hydrazides and *N,N*-heterocyclic ligands (Fig. 1). The new complexes were characterized by elemental analyses, conductivity measurements, high-resolution electrospray ionization mass spectrometry (HRESIMS), FT-IR, UV–Vis and EPR. Thereafter, DNA interactions, pro-apoptotic properties, cytotoxicity and antitubercular activity of the synthesized compounds were evaluated.

2. Experimental

2.1. Starting materials

The reagents (ligands and metallic salts) are commercially available (Sigma-Aldrich).

2.2. Physical measurements

Conductivity studies were carried out with a Tecnal Tec-4MP conductivity meter using a cell of constant 1.03 cm^{-1}. Spectroscopic grade methanol (Sigma-Aldrich) (Λ_M = 2.13 μs/cm) was used as solvent.

Elemental analyses were performed using a Perkin-Elmer 2400 CHN Elemental Analyzer.

Infrared spectra were obtained on a PerkinElmer Spectrum Two spectrophotometer equipped with an attenuated total reflectance (ATR) sample holder and ZnSe crystal. The spectra were recorded in the range of 4000–600 cm^{-1}.

Diffuse reflectance spectra and UV–Vis were obtained on a Shimadzu UV-2501 PC spectrophotometer.

High-resolution electrospray ionization mass spectra (HRESIMS) were measured on an ultrOTOF (Bruker Daltonics) spectrometer, operating in the positive mode. Methanol was used as solvent system and the samples were infused into the ESI source at a flow rate of 5 μL/min. The calculated values for the charged complex ions were made using ChemDraw Ultra 15.0.

To register EPR spectra of the metal complexes, a Bruker instrument (Karlsruhe, Germany) model EMX was used, operating at X-band (9.50 GHz frequency, 20 mW power, 100 kHz modulation frequency), at 77 K. Samples in solid or as frozen methanol solution were used, in Wilmad quartz tubes, and frequency calibration was provided with DPPH (α,α'-diphenyl-β-picrylhydrazyl; g = 2.0036).

2.3. Crystal structure determination

The data collection was performed at room temperature (296 K) using Mo-Kα radiation (λ = 0.71073 Å) on a BRUKER APEX II Duo diffractometer. Standard procedures were applied for data reduction and absorption correction. The structure was solved with SHELXS97 using direct methods [33] and refined by full-matrix least-square methods against F^2 (SHELXL2014) [34]. All non-hydrogen atoms were refined with anisotropic displacement parameters with SHELXL2014 [34]. The hydrogen atoms were calculated at idealized positions using the riding model option of SHELXL2014 [34]. Crystallographic data, experimental details, data collection and refinement are reported in Table 1.

2.4. Preparation of the complexes

All complexes were prepared by the reaction of $Cu(ClO_4)_2{\cdot}6H_2O$

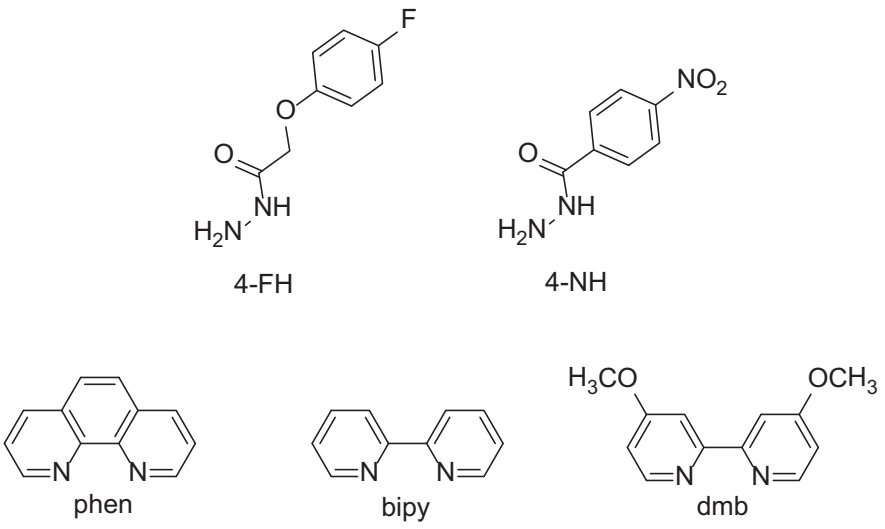

Fig. 1. Organic compounds used as ligands.

Table 1
Crystal data and structure refinement for complex **I**.

Empirical formula	$C_{20}\ H_{17}\ Cl_2\ Cu\ F\ N_4\ O_{10}$
Formula weight	626.82
Temperature	296(2) K
Wavelength	0.71073 Å
Crystal system	Monoclinic
Space group	P 2_1/c
Unit cell dimensions	a = 18.6542(6) Å b = 13.7070(4) Å β = 96.4240(10)° c = 9.2529(3) Å
Volume	2351.05(13) $Å^3$
Z	4
Density (calculated)	1.771 Mg/m^3
Absorption coefficient	1.230 mm^{-1}
F(000)	1268
Crystal size	0.40 × 0.12 × 0.09 mm^3
θ range for data collection	1.098 to 26.394°
Index ranges	−23 < =h < =23, −17 < =k < =17, −11 < =l < =11
Reflections collected	42,766
Independent reflections	4816 [R(int) = 0.0274]
Completeness to theta = 25.242	100.0%
Absorption correction	Multi-scan
Max. and min. Transmission	0.7454 and 0.6596
Refinement method	Full-matrix least-squares on F^2
Data/restraints/parameters	4816/14/381
Goodness-of-fit on F^2	1.043
Final R indices [I > 2sigma (I)]	R_1 = 0.0401, wR_2 = 0.1082
R indices (all data)	R_1 = 0.0473, wR_2 = 0.1138
Extinction coefficient	n/a
Largest diff. Peak and hole	0.687 and −0.547 e.$Å^{-3}$

(0.09 g, 0.25 mmol) with 0.25 mmol of hydrazide dissolved in a minimum amount of methanol. The mixture was stirred for 2 h, followed by the addition of *N,N*-donor heterocyclic ligand (0.25 mmol) previously dissolved in methanol. After 48 h, the compound was filtered, washed with methanol and dried under reduced pressure.

a. $[Cu(4\text{-}FH)(phen)(ClO_4)_2]$ **I.**

M.M.: 626.82 g mol^{-1}. Yield: 75%. Color: Blue. Anal. Calc. for ($CuC_{20}H_{17}FN_4O_{10}Cl_2$): C, 38.32; H, 2.73; N, 8.94%. Found: C, 38.68; H, 2.77; N, 8.90%. (+)-HRESIMS (methanol), *m/z*: 426.0555 [M – $2ClO_4$ – H]$^+$ (calc. For $C_{20}H_{16}CuFN_4O_2$, 426.0548 (Δ 1.6 ppm)). IR (ATR) ν (cm^{-1}): 3262, 3204, 3069, 1661, 1588, 1525, 1511, 1434, 1371, 1250, 1221, 1138, 1100, 1088, 1049, 927, 878, 854, 830, 780, 742, 721, 652, 615. UV–Vis (methanol), λ_{max} (nm) = 293 ($1.1 \times 10^4\ M^{-1}\ cm^{-1}$), 272 ($3.5 \times 10^4\ M^{-1}\ cm^{-1}$), 220 ($3.7 \times 10^4\ M^{-1}\ cm^{-1}$), 640 ($2.9 \times 10^1\ M^{-1}\ cm^{-1}$), 610 (solid). EPR parameters (in methanol frozen solution): $g_\perp$ 2.063; $g_{//}$ 2.255; $A_{//}$ $185 \times 10^{-4}\ cm^{-1}$. Molar conductivity, ΛM (methanol) = 188.45 μS cm^{-1}.

b. $[Cu(4\text{-}FH)(dmb)(ClO_4)_2]\cdot H_2O$ **II**

M.M.: 680.86 g mol^{-1}. Yield: 51%. Color: Blue. Anal. Calc. for ($CuC_{20}H_{23}FN_4O_{13}Cl_2$): C, 35.28; H, 3.40; N, 8.23%. Found: C, 34.85; H, 3.56; N, 7.81%. (+)-HRESIMS (methanol), *m/z*: 462.0760 [M–$2ClO_4$–H]$^+$ (calc. for $C_{20}H_{20}CuFN_4O_4$, 462.0759 (Δ 0.2 ppm)). IR (ATR) ν (cm^{-1}): 3613, 3256, 3094, 2980, 1669, 1614, 1562, 1506, 1476, 1444, 1424, 1370, 1342, 1322, 1288, 1272, 1264, 1251, 1229, 1217, 1087, 1048, 1030, 1010, 970, 920, 889, 859, 832, 778, 742. UV–Vis (methanol), λ_{max} (nm) = 299 ($1.4 \times 10^4\ M^{-1}\ cm^{-1}$), 286 ($1.7 \times 10^4\ M^{-1}\ cm^{-1}$), 277 ($1.8 \times 10^4\ M^{-1}\ cm^{-1}$), 229 ($6.4 \times 10^4\ M^{-1}\ cm^{-1}$), 635 ($2.6 \times 10^1\ M^{-1}\ cm^{-1}$), 607 (solid). EPR parameters (in methanol frozen solution): $g_\perp$ 2.058; $g_{//}$ 2.244; $A_{//}$ $188 \times 10^{-4}\ cm^{-1}$. Molar conductivity, ΛM (methanol) = 176.01 μS cm^{-1}.

c. $[Cu(4\text{-}NH)(phen)(ClO_4)_2]\cdot H_2O$ **III**

M.M.: 641.81 g mol^{-1}. Yield: 54%. Color: Blue. Anal. Calc. for ($CuC_{19}H_{17}N_5O_{12}Cl_2$): C, 35.56; H, 2.67; N, 10.91%. Found: C, 35.95; H, 2.68; N, 10.92%. (+)-HRESIMS (methanol), *m/z*: 423.0399 [M – $2ClO_4$ −H]$^+$ (calc. For $C_{19}H_{14}CuN_5O_3$, 423.0387 (Δ 2.8 ppm)). IR (ATR) ν (cm^{-1}): 3509, 3461, 3236, 3166, 3092, 3070, 2978, 2915, 1653, 1619, 1574, 1522,1493, 1431, 1368, 1350, 1322, 1236, 1160, 1133, 1101, 1088, 1054, 1011, 924, 866, 856, 826, 788, 741, 721, 710. UV–Vis (methanol), λ_{max} (nm) = 293 ($2.\ 2 \times 10^4\ M^{-1}\ cm^{-1}$), 272 ($5.6 \times 10^4\ M^{-1}\ cm^{-1}$), 224 ($4.8 \times 10^4\ M^{-1}\ cm^{-1}$), 206 ($5.1 \times 10^4\ M^{-1}\ cm^{-1}$), 632 ($3.5 \times 10^1\ M^{-1}\ cm^{-1}$), 608 (solid). EPR parameters (in methanol frozen solution): $g_\perp$ 2.062; $g_{//}$ 2.254; $A_{//}$ $183 \times 10^{-4}\ cm^{-1}$. Molar conductivity, ΛM (methanol) = 168.19 μS cm^{-1}.

d. $[Cu(4\text{-}NH)(bipy)(ClO_4)_2]\cdot H_2O$ **IV**

M.M.: 617.79 g mol^{-1}. Yield: 60%. Color: Blue. Anal. Calc. for ($CuC_{17}H_{17}N_5O_{12}Cl_2$): C, 33.05; H, 2.77; N, 11.34%. Found: C, 33.43; H, 2.68; N, 11.12%. (+)-HRESIMS (methanol), *m/z*: 399.0393 [M – $2ClO_4$ – H]$^+$ (calc. For $C_{17}H_{14}CuN_5O_3$, 399.0387 (Δ 1.5 ppm)). IR (ATR) ν (cm^{-1}): 3534, 3475, 3240, 3172, 3116, 3085, 3038, 2979, 2902, 2858, 1650, 1618, 1610, 1601, 1574, 1522, 1496, 1476, 1448, 1348, 1321, 1249, 1227, 1178, 1127, 1110, 1089, 1056, 1034, 1013, 933, 909, 866, 852, 825, 778, 731, 709, 666. UV–Vis (methanol), λ_{max} (nm) = 310 ($2.4 \times 10^4\ M^{-1}\ cm^{-1}$), 298 ($2.7 \times 10^4\ M^{-1}\ cm^{-1}$), 249 ($3.0 \times 10^4\ M^{-1}\ cm^{-1}$), 206 ($3.4 \times 10^4\ M^{-1}\ cm^{-1}$), 203 ($3.6 \times 10^4\ M^{-1}\ cm^{-1}$), 625 ($1.3 \times 10^1\ M^{-1}\ cm^{-1}$), 605 (solid). Molar conductivity, ΛM (methanol) = 191.75 μS cm^{-1}.

e. $[Cu(4\text{-}NH)(dmb)(ClO_4)_2].H_2O$ **V**

M.M.: 677.84 g mol^{-1}. Yield: 73%. Color: Blue. Anal. Calc. for ($CuC_{19}H_{21}N_5O_{14}Cl_2$): C, 33.67; H, 3.12; N, 10.33%. Found: C, 33.40; H, 2.97; N, 10.00%. (+)-HRESIMS (methanol), *m/z*: 459.0606 [M – $2ClO_4$ – H]$^+$ (calc. for $C_{19}H_{18}CuN_5O_5$, 459.0598 (Δ 1.7 ppm)). IR (ATR) ν (cm^{-1}): 3610, 3257, 3180, 3125, 3090, 2972, 2912, 2848, 1652, 1609, 1573, 1558, 1533, 1499, 1474, 1440, 1417, 1347, 1323, 1283, 1251, 1222, 1128, 1093, 1063, 1044, 1013, 970, 931, 907, 871, 852, 838, 709. UV–Vis (methanol), λ_{max} (nm) = 299 ($2.7 \times 10^4\ M^{-1}\ cm^{-1}$), 287 ($3.2 \times 10^4\ M^{-1}\ cm^{-1}$), 229 ($8.4 \times 10^4\ M^{-1}\ cm^{-1}$), 622 ($7.1\ M^{-1}\ cm^{-1}$), 604 (solid). Molar conductivity, ΛM (methanol) = 214.60 μS cm^{-1}.

2.5. Cells and culture

2.5.1. K562 cells

The K562 cell line was purchased from the Rio de Janeiro Cell Bank (number CR083 of the RJCB collection). This cell line was established from pleural effusion of a 53 year-old female with chronic myelogenous leukemia in terminal blast crisis. Cells were cultured in RPMI 1640 (Sigma Chemical Co.) medium supplemented with 10% fetal calf serum (CULTILAB, São Paulo, Brazil) at 37 °C in a humidified 5% CO_2 atmosphere. Cultures grow exponentially from 10^5 cells mL^{-1} to about 8×10^5 cells mL^{-1} in three days. Cell viability was checked by Trypan Blue exclusion. The cell number was determined by Coulter counter analysis.

For cytotoxicity assessment, 1×10^5 cells mL^{-1} were cultured for 72 h in the absence and presence of a range of concentrations of tested compounds. The sensitivity to compound was evaluated by the concentration that inhibits cell growth by 50% (IC_{50}). Stock solutions were prepared in DMSO and diluted accordingly to obtain the concentrations used in the cytotoxic assays. The final concentration of

DMSO in the experiments was below 0.5% and we have checked that the solvent has no effect in cell growth at this concentration.

2.5.2. Human breast cancer cell lines

The MDA-MB-231 and MCF-7 cell lines were purchased from the Rio de Janeiro Cell Bank. MCF-7 and MDA-MB-231 cells were cultured in DMEM medium supplemented with 10% fetal bovine serum, 100 units/mL penicillin, 100 mg/mL streptomycin, pH 7.4 at 37 °C with 5% CO_2, in humid chamber, to reach ≈80% confluence for assays. Cells detachments for subculture/plating were done with a trypsin/EDTA solution for MCF-7 cells and EDTA solution for MDA-MB-231 cells, for 5 min; trypsin inactivation was carried out with BFS when applied and the cells were washed three times with medium. The cell number was determined by Neubauer chamber Counter analysis.

For cytotoxicity assessment, 5×10^4 cells mL^{-1} were cultured for 36 h in the absence and the presence of a range of concentrations of tested compounds. The sensitivity to compound was evaluated by the concentration that inhibits cell growth by 50% (IC_{50}). Stock solutions of the compounds were prepared in DMSO.

2.5.3. Determination of cell death mode – flow cytometric analysis

The Annexin V/Dead Cell kit utilizes a fluorescent dye conjugated to Annexin-V to detect phosphatidylserine on the external membrane of apoptotic cells and a cell death dye 7-AAD that provides information on the membrane integrity or cell death. 7-AAD is excluded from living healthy cells, as well as early apoptotic cells. By observing the events of graphical plots populations of cells were classified into four distinguished groups: *Viable cells*: Annexin (−) and 7-AAD (−), lower-left quadrant (Q_4); *Early apoptotic cells*: Annexin (+) and 7-AAD (−), lower right quadrant (Q_3); *Late apoptotic cells*: Annexin (+) and 7-AAD (+), upper-right quadrant (Q_2). *Cells that have died through non-apoptotic pathway*: Annexin V (−) and 7-AAD (+), upper-left quadrant (Q_1). MDA-MB-231 cells were seeded in a 24-well culture plate at a density of 3×10^5 cells/well and were cultured overnight in RPMI supplemented with 5% fetal bovine serum. In the next day cells were exposed to 50 μM of the complexes **I** and **III** for 24 h. MDA-MB-231 cells were harvested by trypsinisation and analyzed for the detection of early/late apoptosis and cell death mode using Annexin V/Dead Cell and 7-AAD.

2.6. Anti-Mycobacterium tuberculosis activity assay

The anti-MTB activity of the compounds was determined by the REMA (Resazurin Microtiter Assay) method [35]. Stock solutions of the tested compounds were prepared in DMSO at 10 mg/mL and diluted in Middlebrook 7H9 broth (Difco) supplemented with oleic acid, albumin, dextrose and catalase (OADC), performed by Precision XS (Biotek®) to obtain the final drug concentration range of 0.09–25 μg/mL. Rifampicin was dissolved in DMSO and was used as standard drugs. A suspension of the *M. tuberculosis* H37Rv ATCC 27294 was cultured in Middlebrook 7H9 broth supplemented with OADC and 0.05% Tween 80. When the culture obtained a turbidity of McFarland standard No. 1, it was adjusted by 5×10^5 CFU per mL and 100 μL of the inoculum were added to each well of a 96-well microplate (Kasvi®) together with 100 μL of the compounds. Samples were set up in triplicate. The plates were incubated for 7 days at 37 °C. Resazurin (solubilized in water) was added (30 μL of 0.01%). The fluorescence of the wells was read after 24 h with a Cytation 3 (Biotek®). The MIC was defined as the lowest concentration resulting in 90% inhibition of growth of MTB.

2.7. DNA binding

A Cary100 Varian spectrometer was used for UV and visible absorption measurements. For the interactions with CT DNA, the complex concentration used was 2.5×10^{-5} M and the DNA concentration varied from 0 to 3×10^{-4} M. The DNA concentration per nucleotide was determined by the $\varepsilon = 6600\ M^{-1}\ cm^{-1}$ at 260 nm. The ionic strength was maintained constant with 1×10^{-3} M NaCl and the pH was fixed at 7.3 with 20 mM HEPES buffer. The absorbance of DNA itself was subtracted by adding equal quantity of DNA to both the complex and the reference solutions.

CD spectra were recorded in a Jasco J-815 spectropolarimeter in HEPES buffer (20×10^{-3} M) pH 7.3. DNA concentration was 1×10^{-4} M and complex concentration varied from 0 to 3.2×10^{-5} M. The absorbance of the complexes was subtracted from that of the reaction mixture.

3. Results and discussion

Ternary complexes of copper(II) of the type $[Cu(N{-}O)(N{-}N)(ClO_4)_2]$, in which N–O = 4-fluorophenoxyacetic acid hydrazide (4-FH) or 4-nitrobenzoic hydrazide (4-NH); N–*N* = 1,10-phenanthroline (phen), 4–4′-dimethoxy-2-2′-bipyridine (dmb) or 2,2-bipyridine (bipy) were synthesized. The complexes were characterized by elemental analyses, conductivity measurements and spectroscopic methods. In addition, complex **I** was analyzed by single crystal X-ray diffraction. All the copper complexes are colorful, non-hygroscopic, stable to air and light and soluble in organic solvents such as methanol, DMSO and acetonitrile.

The results of elemental analyses, which are given in experimental section, are in accordance with the proposed structures. The molar conductance measurements of the complexes were performed in methanol (1×10^{-3} M) at room temperature. The values varied between 168.19 and 214.60 μS cm^{-1}, depending of the complex, which indicates that they are 1:2 electrolytes [31]. The labilization of the axial ligands in solution (perchlorate anions) results in the generation of compounds of type $[Cu(N{-}O)(N{-}N)]^{2+}$ [17,19].

The high-resolution mass spectra of the copper complexes were recorded. The water molecules present in the molecular structures of **II–V** were dissociated from the complexes in the ionization process. The *m/z* values listed in the experimental section refer to the peak containing the most abundant isotope (^{63}Cu). For instance, mass spectrum of the complex **V** exhibited the charged ion at *m/z* 459.0606 $[M–2ClO_4–H]^+$ that was close to the calculated value for $C_{19}H_{18}CuN_5O_5$, 459.0598 (Δ 1.7 ppm), and represents the pattern observed for all compounds (Fig. 2) [36].

In the IR spectra of the complexes **II–V**, a broad band at 3550 cm^{-1} indicates the presence of one water molecule. For all complexes, a group of bands between 2900 and 3080 cm^{-1} corresponds to the νC–H stretching vibration. Two intense bands between 1085 and 1045 cm^{-1} are attributable to the presence of two unidentate perchlorate ions [37]. Hydrazides show characteristic absorptions between 3332 and 3150 cm^{-1} which are attributable to the NH_2 and NH groups [22,23]. In all complexes studied, the bands originating from NH_2 group showed considerable shift as compared to the free ligands. An absorption assigned to νC═O around 1666–1645 cm^{-1} corroborates with the proposed structures.

Electronic absorption spectra of all compounds were performed in methanol (10^{-5} M). A red shift in relation to free ligands confirms the presence of the complexes in solution [31]. The complexes possess only one broad and asymmetric d-d band centered at ≈630 nm. For example, the complex **IV** exhibits a d-d band centered at 625 nm ($\varepsilon = 13\ M^{-1}\ cm^{-1}$). These observations are consistent with a distortion from the octahedron geometry due to the Jahn-Teller effect [19]. In the solid state, all complexes exhibit the same d-d band centered at ≈608 nm, indicating that the geometry of the complexes in solution differs from that in solid state [19,20]. Moreover, in the solid state, the complexes exhibited a new band (CT) around 480 nm.

From EPR data, the corresponding parameters were determined for the studied copper(II) complexes (Table 2). The obtained values were very close, indicating a tetragonal arrangement of the ligands around the copper center, with a small tetrahedral distortion, as estimated by the empirical ratio $g_{//}/A_{//}$ [31], around 120 cm. In the solid state, all

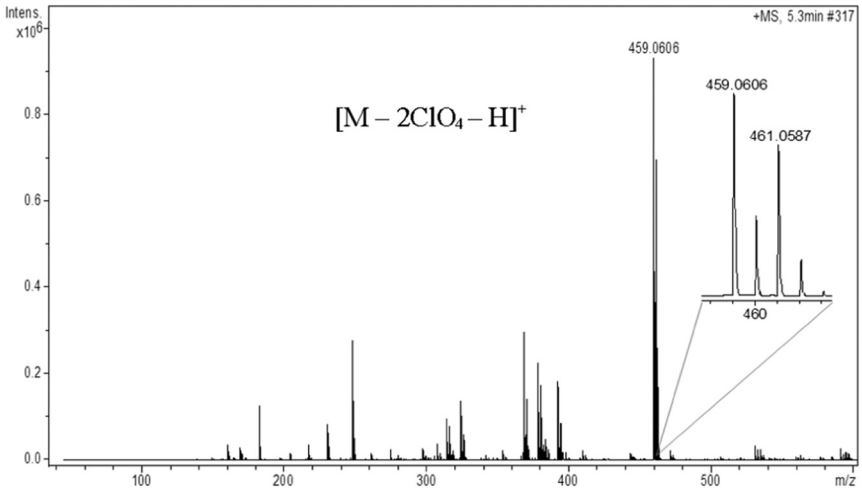

Fig. 2. (+)-HRESI-MS spectrum of complex **V** (charged complex ion observed was $[M - 2ClO_4 - H]^+$).

Table 2
EPR parameters for copper(II) complexes in solid state and in methanol frozen solution, at 77 K.

Complex	g_{iso}[#]	$g_{\perp}$	$g_{//}$	$A_{//}$ (G)	$A_{//}$ (10^{-4} cm^{-1})[§]	$g_{//}$ /$A_{//}$ (cm)
I	2.065	2.063	2.255	176	185	122
II	2.065	2.058	2.244	179	188	119
III	2.071	2.062	2.254	174	183	123

[#] In solid state.
[§] $\mathbf{A}_{//}$ (in 10^{-4} cm^{-1}) = $g_{//}$ β $A_{//}$ (in G) = 0.46686 × 10^{-4} $g_{//}$ $A_{//}$ (in G); where β = 1.39969 MHz/G.

the compounds exhibited only an isotropic g_{iso} value, 2.065 to 2.071.

3.1. Crystal structure

Blue crystals suitable for single crystal X-ray diffraction were obtained for complex **I** after slow evaporation of a methanol/toluene solution at room temperature. The crystals thereby formed were collected, washed with water and dried under reduced pressure. Single crystal X-ray analysis demonstrates that complex **I** crystallizes in the monoclinic system, space group $P2_1/c$. Fig. 3 illustrates the molecular structure of the complex **I** along with atomic labeling scheme. As it can be seen, the complex **I** exhibits a distorted octahedral geometry around Cu(II) ion, in which the ligands are coordinated in a bidentate mode. The equatorial site is occupied by two nitrogen atoms from phen (N3 and N4) and two atoms from 4-FH ligand (O1 and N2). The apical sites are occupied by two oxygen atoms (O3a and O10a) from two perchlorates weakly bonded [31]. The perchlorate anions are disordered over two sites. The solid lines (labeled a) indicate the bonds between the atoms with higher occupation factor (54.7%), whereas the dashed lines (labeled b) represent the species with the lower occupation (45.3%). Selected bond lengths and angles are reported in Table 3.

The Cu1—O bond lengths from the disordered perchlorate ions range from 2.4 to 2.8 Å. These values are considerably longer than the Cu1—O distance in the basal plane. This elongation can be explained by the Jahn-Teller effect [19]. The Cu1—N_{phen} (1.994(2) and 1.976(2)Å), Cu1—N2 (2.025(2) Å) and Cu1—O1 (1.970(2) Å) bond distances are normal and are comparable to those found for the related copper(II) complexes [31,38–41].

The basal geometry is considerably distorted from the perfect square-plane owing to the bite angle of the chelating phen ligand (83.23(9)°). The *trans* angles are 173.20(9)° and 174.52(9)°. The values of bond lengths and angles are within the values expected for this class of compounds [31,38]. The bidentate chelation to the copper(II) ion by the ligands lead to the formation of two 5-membered planar rings and the root mean square (r.m.s) deviation to the fitted atoms is 0.0154 and 0.0124 Å. The angle between the mean planes formed by these rings is 7.27(13)°. The copper atom is in the equatorial plane and the r.m.s deviations of the five fitted atoms in the CuN3O plane are 0.0368 Å. The phen ligand is approximately planar and the r.m.s deviations to the fitted non-hydrogen atoms are 0.0251 Å. The copper ion is displaced about 0.050 Å in relation to this plane.

The crystal structure is stabilized by hydrogen bonds (listed in Table 4) and weak π–π stacking interactions. Intramolecular hydrogen bonds could be observed between the donor atoms of the 4-FH ligand and the oxygen atoms of the perchlorate groups (N2⋯O8a = 2.987(8)

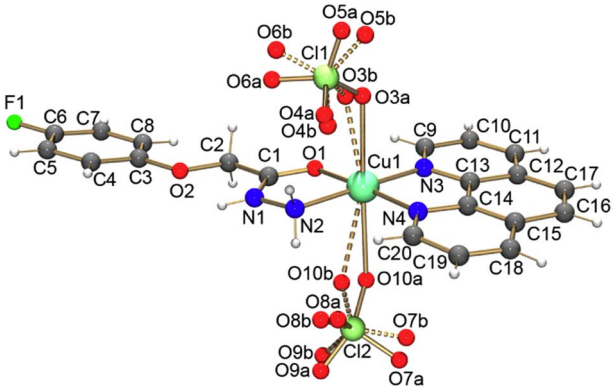

Fig. 3. Molecular structure of the complex $[Cu(4\text{-}FH)(phen)(ClO_4)_2]$ **I** showing oxygen atoms from the perchlorate disordered over two sites. Major component (solid lines) with 54.7% occupation and minor component (dashed lines) with 45.3% occupation.

Table 3
Select bond lengths [Å] and angles [°] for complex **I**.

Cu1—O1	1.970(2)
Cu1—N2	2.025(2)
Cu1—N3	1.976(2)
Cu1—N4	1.994(2)
Cu1—O3a	2.489(7)
Cu1—O3b	2.412(10)
Cu1—O10a	2.601(7)
Cu1—O10b	2.769(7)
N3—Cu1—N4	83.23(9)
O1—Cu1—N2	82.49(8)
N4—Cu1—N2	100.89(9)
O1—Cu1—N3	93.04(8)
O1—Cu1—N4	173.20(9)
N3—Cu1—N2	174.52(9)

Table 4
Hydrogen bonds for complex **I** [Å and °].

D—H···A	d(D—H)	d(H···A)	d(D···A)	< (DHA)
N1—H1···O8a$^{\#1}$	0.86	2.38	2.846(7)	114.3
N1—H1···O9a$^{\#1}$	0.86	2.38	3.212(11)	163.7
N1—H1···O8b$^{\#1}$	0.86	2.14	2.723(8)	124.9
N2—H2a···O8a	0.89	2.18	2.987(8)	150.2
N2—H2a···O8b	0.89	2.07	2.881(9)	151.5
N2—H2b···O4a	0.89	2.40	3.164(12)	143.8
N2—H2b···O4b	0.89	2.20	2.955(12)	141.7

Symmetry transformations used to generate equivalent atoms: #1 x, − y + 1/2, z-1/2.

Å and N2···O4a = 3.164(12) Å) as illustrated in Fig. S1 (Supplementary Material). The N1 nitrogen atom of the 4-FH ligand is a proton donor in two hydrogen bonds of the type N—H···O, involving the O8 and O9 oxygen atoms from perchlorate groups, resulting in chains that extend along [001] direction as depicted in Fig. S2 (Supplementary Material). Using complete graph-set analysis [42] to describe patterns in the hydrogen-bond network, we find $C_1^2(7)[R_1^2(4)]$. These chains connect into a three-dimensional architecture by π–π stacking interactions among the phen moieties belonging to adjoining layers with centroid–centroid (Cg1–Cg2) distance of 3.770(1) Å for Cg1 (generated by the ring C9/C10/C11/C12/C13/N3) and Cg2 (generated by ring C12–C17) (Fig. S3, Supplementary Material).

3.2. Behavior in aqueous solution

The complexes were evaluated by UV–Vis spectroscopy at different times in a mixture containing H_2O/DMSO 0.1%. The values of absorbance and wavelength were not affected, even after 6 h. These results indicate that the species $[Cu(N—O)(N—N)]^{2+}$ remain intact in solution under the test conditions [19]. The spectra of a representative complex are reported in the Fig. 4.

3.3. Cytotoxic studies and determination of cell death mode

The cytotoxic activity of complexes is depicted in Table 5. IC_{50} values obtained for the free ligands, carboplatin and for the complex $[Cu(phen)_2](ClO_4)_2$ are also shown for the sake of comparison.

Concerning K562 cell line, phen and 4-NH exhibit high activity. However, for the phenanthroline and its derivatives, it is assumed that the sequestering of trace metals *in situ* is involved and that the resulting metallic complexes are the active species [43]. The organic compounds bipy and dmb display moderate activity. In turn, the copper complexes inhibit the growth of K562 cells with IC_{50} values between 1.6 and 28 μM. As can be seen in the Table 5, the order of cytotoxic activity is: **III** > **I** > **V** > **II** > **IV**. The copper complexes with 1,10-phenanthroline (phen) are more active than those with 4–4′-dimethoxy-2-2′-bipyridine (dmb) and 2,2-bipyridine (bipy). In the literature, several studies have shown that copper(II) complexes with phenanthroline are more reactive than similar ones with bipyridine ligands [17,31,44]. An accepted explanation for this order of reactivity is that the planar polycyclic phen ring interacts better with DNA [45]. The cytotoxic activity of complexes **I** and **III** is higher than the activity of all corresponding free ligands, carboplatin and $[Cu(Phen)_2]^{2+}$, a complex known by its nuclease action [31]. The complexes **II**, **IV** and **V** exhibit moderate to good activity against K562 cell line.

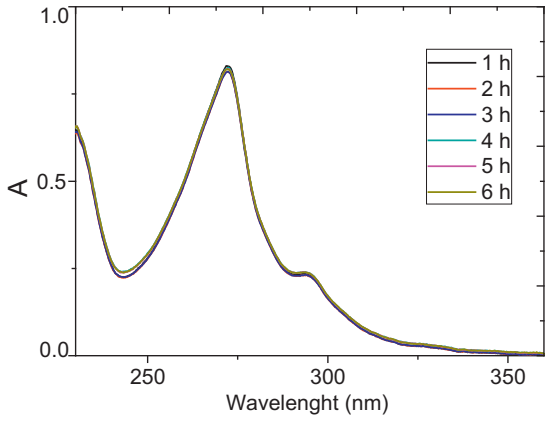

Fig. 4. Ultraviolet spectra of complex **I** as a function of time.

Table 5
IC_{50} (μM) values for ligands, complexes, $[Cu(phen)_2](ClO_4)_2$ and carboplatin.[a]

Compound	K562 (72 h)	MDA-MB-231 (36 h)	MCF-7 (36 h)
4-FH	> 100	> 100	> 100
4-NH	10.5	> 100	> 100
dmb	23.5	–	–
bipy	30.0	–	–
phen	3.2	> 100	> 100
$[Cu(4\text{-}FH)(phen)(ClO_4)_2]$ **I**	1.8	8.8	6.5
$[Cu(4\text{-}FH)(dmb)(ClO_4)_2].H_2O$ **II**	26.2	–	–
$[Cu(4\text{-}NH)(phen)(ClO_4)_2].H_2O$ **III**	1.6	5.5	4.6
$[Cu(4\text{-}NH)(bipy)(ClO_4)_2].H_2O$ **IV**	28.0	–	–
$[Cu(4\text{-}NH)(dmb)(ClO_4)_2].H_2O$ **V**	15.0	–	–
$[Cu(phen)_2](ClO_4)_2$	3.4	–	–
Carboplatin	10.0	> 100	> 100

[a] IC_{50} is the concentration required to inhibit 50% of K562 cell growth.

As it can be seen in Table 5, the complexes **I** and **III** were also very active against MDA-MB-231 and MCF-7 cells. It is worth noting that the free ligands and carboplatin exhibit IC_{50} values > 100 μM against MDA-MB-231 and MCF-7 cells. In general, the cytotoxic activity of these compounds is similar to copper complexes with *N,N*-donor heterocyclic ligands already described [46–51,17,31], although, the mode of action can be quite different [19].

We have used flow cytometric analysis to determine whether the selected complexes **I** and **III** (50 μM) are able to induce apoptosis. In accordance with our results, after 24 h incubation, the copper complexes **I** and **III** induce late apoptosis in MDA-MB-231 cell line (Fig. 5). Several copper(II) complexes were reported in literature by induce apoptosis, a form of programmed cell death that occurs in tumor cells as response to some anticancer agents [52–54].

3.4. DNA binding

We have registered the spectra of solutions of the complexes in the absence and in the presence of increasing concentrations of CT DNA. The addition of DNA induces a hypochromic effect and a minor batochromic shift, indicating that both complexes interact with calf thymus DNA. A representative experiment obtained with complexes **I** and **III** at 2.5×10^{-5} M and DNA concentration ranging from 0 a 3×10^{-4} M is shown in Figs. 6 and 7, respectively. In order to evaluate the binding strengths of the complexes, the binding constant, K, was calculated accordingly to the equation.

$$[DNA] / (\varepsilon_a - \varepsilon_f) = [DNA] / (\varepsilon_0 - \varepsilon_f) + 1/K(\varepsilon_0 - \varepsilon_f).$$

in which, [DNA] is the concentration of DNA in base pairs, ε_a is the ratio of the absorbance/[Cu], ε_f is the extinction coefficient of the free Cu^{II} complex and ε_0 is the extinction coefficient of the complex in the fully bound form. The ratio of slope to intercept in the plot of [DNA]/($\varepsilon_a - \varepsilon_f$) *versus* [DNA] gives the value of K (Figs. 6 and 7). The affinity of complex **I** to DNA is slightly higher than that complex **III** with K values of 4.38×10^4 and 2.62×10^4, respectively.

The high sensitivity of circular dichroism (CD) to conformational aspects makes this technique suitable to follow changes in DNA

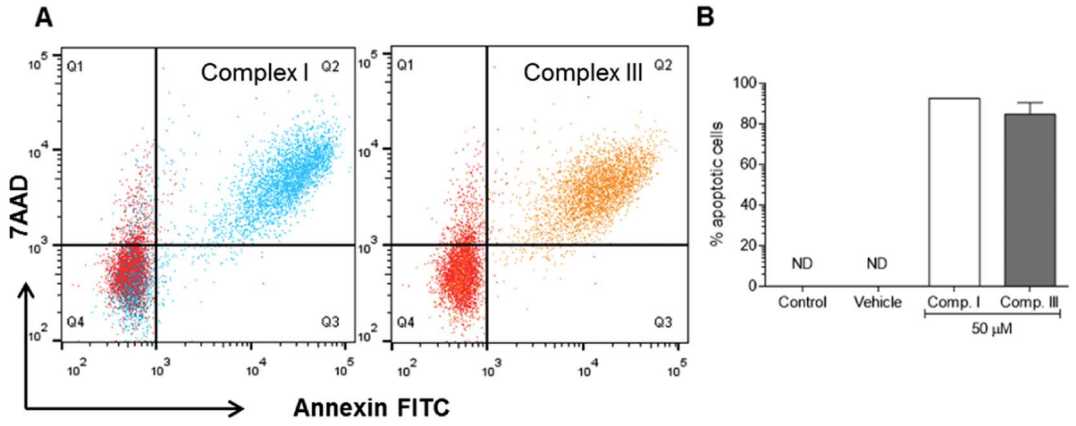

Fig. 5. Representative flow cytometry plots of MDA-MB-231 cell treated with complexes **I** and **III**.

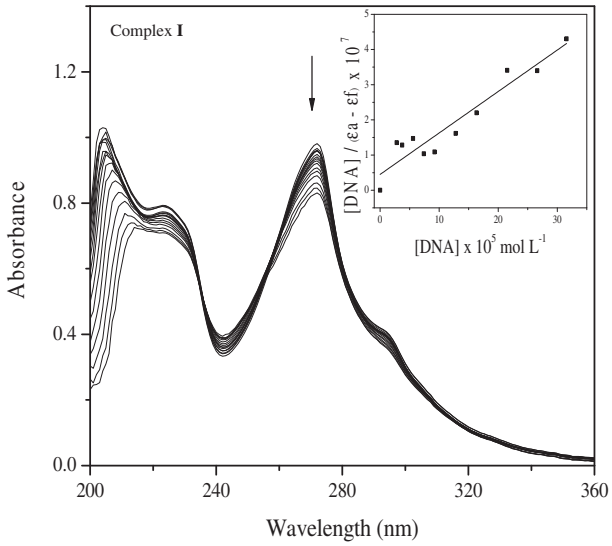

Fig. 6. Spectra of solutions containing complex **I** (2.5×10^{-5} M) and increasing concentrations of DNA in HEPES buffer pH 7.3. [DNA]: [complex **I**] ranging from 0 to 12. Inset: [DNA]/(εa - εf) *versus* [DNA].

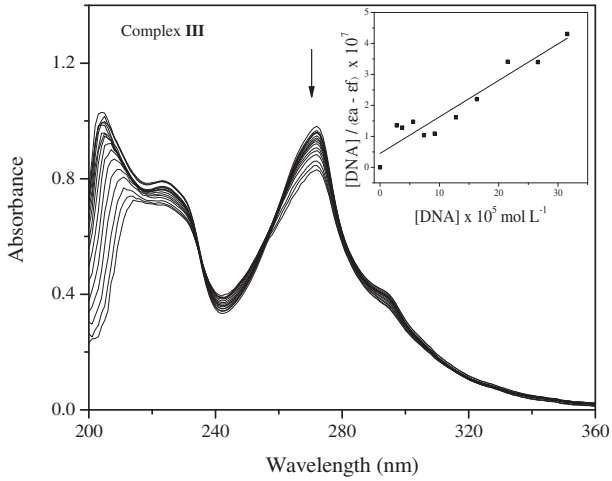

Fig. 7. Spectra of solutions containing complex **III** (2.5×10^{-5} M) and increasing concentrations of DNA in HEPES buffer pH 7.3. [DNA]: [complex **III**] ranging from 0 to 12. Inset: [DNA]/(εa - εf) *versus* [DNA].

morphology caused by interactions with drugs or small molecules. The CD spectrum of the free DNA is composed of a positive band at 275 nm, due to base stacking, and a negative one at 245 nm, due to the right-handed helicity of B-DNA [55–56]. By adding aliquots of **I** and **III** in the DNA solution the intensity of DNA bands increase (Fig. S4). This behavior is usually observed upon drug intercalation, since it enhances the base stacking and stabilizes helicity, and thus increases intensities of the bands, whereas simple groove binding and electrostatic interaction of small molecules show less or no perturbation on the base stacking and helicity bands [55–56].

3.5. Anti-*M. tuberculosis* activity

The antimycobacterial activity of compounds **I** and **III** were evaluated *in vitro* against MTB H37Rv (ATCC 27294) strain by the REMA method. The minimum inhibitory concentrations (MICs) found for the complexes, free ligands and rifampicin (standard drug) are shown in Table 6. The complexes **I** and **III** exhibited activity against the MTB with MIC values equal to 6.3 and 6.5 μg/mL, respectively. It is worth noting that the novel complexes possess MIC (μM) values lower than those of the corresponding free ligands. Moreover, compared to similar compounds containing aromatic diimine ligands (N—N) already described, they are among the most active [57–59]. Whereas compounds with anti-MTB activity at ≤ 10 μg/mL (or molar equivalent) are selected for subsequent tests [60], these results show that copper complexes containing hydrazides and *N,N*-donor ligands are promising agents against MTB.

4. Concluding remarks

Five new copper complexes containing hydrazides and *N,N*-donor heterocyclic ligands were prepared and characterized. The X-ray structural analysis of one representative compound indicates that the geometry around the copper ion is octahedral distorted, in which both the ligands are coordinated in a bidentate mode, (N—O) and (N—N). EPR parameters determined for the all series of complexes corroborated these data, attesting a tetragonal geometry around the copper ion in solution. The obtained results of cytotoxicity activity of the synthesized compounds are very promising, especially in the case of copper

Table 6
Anti-MTB activity (MIC) of **I**, **III**, free ligands and rifampicin.

Compound	MIC_{90} μg/mL	MIC_{90} μM
phen	2.3	12.7
4-FH	> 25	–
4-NH	> 25	–
$[Cu(4\text{-}FH)(phen)(ClO_4)_2]$ **I**	6.3	10.0
$[Cu(4\text{-}NH)(phen)(ClO_4)_2].H_2O$ **III**	6.5	10.1
Rifampicin (standard drug)	0.02	0.03

complexes with phenanthroline, with IC_{50} values in the range of a few μM. Also, the coordination to the metal ion ameliorates the ligand activity. Regarding its antitubercular activity, they are among the most active in comparison to similar compounds, with MIC ≤ 10 μg/mL. These findings are noteworthy and motivate further studies with such compounds.

Abbreviations

Phen	1,10-phenanthroline
bipy	2,2′-bipyridine
dmb	4–4′-dimethoxy-2-2′-bipyridine
DNA	Deoxyribonucleic acid
CT DNA	calf-thymus DNA
UV–Vis	ultraviolet-visible
IR	infrared
EPR	electron paramagnetic resonance
CD	circular dichroism
DMSO	dimethyl sulfoxide
K562	chronic myelogenous leukemia
MCF-7	breast adenocarcinoma
MDA-MB-231	human breast adenocarcinoma
IC_{50}	concentration required to inhibit 50% of cell growth
MIC	minimum inhibitory concentration
MTB	Mycobacterium tuberculosis
CT	charge transfer

Acknowledgements

To CNPq (Conselho Nacional de Desenvolvimento Científico e Tecnológico, Brazil) (442328/2014-1), CAPES (Coordenação de Aperfeiçoamento de Pessoal de Nível Superior, Brazil), and FAPEMIG (Fundação de Amparo à Pesquisa de Minas Gerais, Brazil) (APQ-00668-15) by financial support and fellowships. The authors are also thankful to the Grupo de Materiais Inorgânicos do Triângulo - GMIT research group supported by FAPEMIG (APQ-00330-14). This work is a collaboration research project of members of the Rede Mineira de Química (RQ-MG) supported by FAPEMIG (Project: CEX - RED-00010-14).

Appendix A. Supplementary data

CCDC 1499893 contains the supplementary crystallographic data for the complex **I**. These data can be obtained free of charge *via* http://www.ccdc.cam.ac.uk/conts/retrieving.html, or from the Cambridge Crystallographic Data Centre, 12 Union Road, Cambridge CB2 1EZ, UK; fax: (+44) 1223-336-033; or e-mail: deposit@ccdc.cam.ac.uk. Supplementary data associated with this article can be found in the online version, at http://dx.doi.org/10.1016/j.jinorgbio.2017.04.024.

References

[1] M. Chikira, C. Hee Ng, M. Palaniandavar, Int. J. Mol. Sci. 16 (2015) 22754–22780.
[2] P. Ruíz, R. Ortiz, L. Perelló, G. Alzuet, M. González-Álvarez, M. Liu-González, F. Sanz-Ruíz, J. Inorg. Biochem. 101 (2007) 831–840.
[3] P.R. Reddy, A. Shilpa, N. Raju, P. Raghavaiah, J. Inorg. Biochem. 105 (2011) 1603–1612.
[4] A.K. Patra, S. Roy, A.R. Chakravarty, Inorg. Chim. Acta 362 (2009) 1591–1599.
[5] I. Correia, S. Roy, C.P. Matos, S. Borovic, N. Butenko, I. Cavaco, F. Marques, J. Lorenzo, A. Rodríguez, V. Moreno, J.C. Pessoa, J. Inorg. Biochem. 147 (2015) 134–146.
[6] A.M. Thomas, A.D. Naik, M. Nethaji, A.R. Chakravarty Inorg, Chim. Acta 357 (2004) 2315–2323.
[7] C. Marzano, M. Pellei, F. Tisato, C. Santini, Anti Cancer Agents Med. Chem. 9 (2009) 185–211.
[8] C. Santini, M. Pellei, V. Gandin, M. Porchia, F. Tisato, C. Marzano, Chem. Rev. 114 (2014) 815–862.
[9] J.L. García-Giménez, M. González-Álvarez, M. Liu-González, B. Macías, J. Borrás, G. Alzuet, J. Inorg. Biochem. 103 (2009) 923–934.
[10] T. Kiran, V.G. Prasanth, M.M. Balamurali, C.S. Vasavi, P. Munusami, K.L. Sathiyanarayanan, M. Pathak, Inorg. Chimica Acta 433 (2015) 26–34.
[11] T. Ma, J. Xu, Yuan Wang, H. Yu, Y. Yang, Y. Liu, W. Ding, W. Zhu, R. Chen, Z. Ge, Y. Tan, L. Jia, T. Zhu, J. Inorg. Biochem. 144 (2015) 38–46.
[12] P. Gurumoorthy, D. Mahendiran, D. Prabhu, C. Arulvasu, A.K. Rahiman, J. Mol. Struct. 1080 (2015) 88–98.
[13] S. Abdolmaleki, M. Ghadermazi, A. Fattahi, S. Sheshmani, Inorg. Chimica Acta 443 (2016) 284–298.
[14] I. Castillo, M. Suwalsky, M.J. Gallardo, V. Troncoso, B.N. Sánchez-Eguía, E. Santiago-Osorio, I. Aguiñiga, A.K. González-Ugarte, J. Inorg. Biochem. 156 (2016) 98–104.
[15] J. Serment-Guerrero, P. Cano-Sanchez, E. Reyes-Perez, F. Velazquez-Garcia, M. Bravo-Gomez, L. Ruiz-Azuara, Toxicol. in Vitro 25 (2011) 1376–1384.
[16] S. Iglesias, N. Alvarez, M.H. Torre, E. Kremer, J. Ellena, R.R. Ribeiro, R.P. Barroso, A.J. Costa-Filho, M.G. Kramer, G. Facchin, J. Inorg. Biochem. 139 (2014) 117–123.
[17] P.P. Silva, W. Guerra, J.N. Silveira, A.M. Da Costa Ferreira, T. Bortolotto, F.L. Fischer, H. Terenzi, A. Neves, E.C. Pereira-Maia, Inorg. Chem. 50 (2011) 6414–6424.
[18] T. Bortolotto, P.P. Silva, A. Neves, E.C. Pereira-Maia, H. Terenzi, Inorg. Chem. 50 (2011) 10519–10521.
[19] J.C. Almeida, D.A. Paixão, I.M. Marzano, J. Ellena, M. Pivatto, N.P. Lopes, A.M. Da Costa Ferreira, E.C. Pereira-Maia, S. Guilardi, W. Guerra, Polyhedron 89 (2015) 1–8.
[20] P.S. Lopes, D.A. Paixão, F.C.S. de Paula, A.M. Da Costa Ferreira, J. Ellena, S. Guilardi, E.C. Pereira-Maia, W. Guerra, J. Mol. Struct. 1034 (2013) 84–88.
[21] S. Rollas, Ş.G. Küçükgüzel, Molecules 12 (2007) 1910–1939.
[22] L.M. Sousa, P.P. Corbi, A.L.B. Formiga, Marcelo Lancellotti, I.M. Marzano, E.C. Pereira-Maia, G. Von Poelhsitz, W. Guerra, J. Mol. Struct. 1097 (2015) 15–22.
[23] M.A. Rodrigues, I.M. Marzano, G.H. Ribeiro, L. Colina-Vegas, M. Pivatto, A.P.S. Fontes, C.M. Ribeiro, F.R. Pavan, K.J. Almeida, A.A. Batista, E.C. Pereira-Maia, W. Guerra, Polyhedron 98 (2015) 146–153.
[24] E.H.S. Sousa, F.G.M. Vieira, J.S. Butler, L.A. Basso, D.S. Santiago, I.C.N. Diógenes, L.G.F. Lopes, P.J. Sadler, J. Inorg. Biochem. 140 (2014) 236–244.
[25] E.H.S. Sousa, L.A. Basso, D.S. Santos, I.C.N. Diógenes, E. Longhinotti, L.G.F. Lopes, I.S. Moreira, J. Biol. Inorg. Chem. 17 (2012) 275–283.
[26] S.A. Galal, K.H. Hegab, A.S. Kassab, M.L. Rodriguez, S.M. Kerwin, A. Abdel-Mo'men, El-Khamry, H.I. El Diwani, Eur. J. Med. Chem. 44 (2009) 1500–1508.
[27] V. Mahalingam, N. Chitrapriya, M. Zeller, K. Natarajan, Polyhedron 28 (2009) 1532–1540.
[28] P. Sur, S.P. Chatterjee, P. Roy, B. Sur, Cancer Lett. 94 (1995) 27–32.
[29] G.D. de Souza, M. A, L.E. Fernandes, P.P. Silva, R. Ruggiero, E.C. Pereira-Maia, W. Guerra, Cent. Eur. J. Chem. 11 (2013) 290–294.
[30] N. Dodoff, K. Granharov, N. Spassovska, J. Inorg. Biochem. 60 (1995) 257–266.
[31] P.P. Silva, W. Guerra, G.C. dos Santos, N.G. Fernandes, J.N. Silveira, A.M. da Costa Ferreira, T. Bortolotto, H. Terenzi, A.J. Bortoluzzi, A. Neves, E.C. Pereira-Maia, J. Inorg. Biochem. 132 (2014) 67–76.
[32] T. Bortolotto, P.P. Silva-Caldeira, C.T. Pich, E.C. Pereira-Maia, H. Terenzi, Chem. Commun. 52 (2016) 7130–7133.
[33] G.M. Sheldrick, SHELXS97, Program for the Solution of Crystal Structures, University of Göttingen, Germany, 1997.
[34] G.M. Sheldrick, SHELXL2014.
[35] J.C. Palomino, A. Martin, M. Camacho, H. Guerra, J. Swings, F. Portaels, Antimicrob. Agents Chemother. 46 (2002) 2720–2722.
[36] K. Shin-Geol Kang, Ryu, Soo-Kyung Jung, Shang-Su Kim, Bull. Kor. Chem. Soc. 17 (1996) 331–334.
[37] S. Dey, T. Mukherjee, S. Sarkar, H.S. Evans, P. Chattopadhyay, Transit. Met. Chem. 36 (2011) 631–636.
[38] K. Kaabi, M. El Glaoui, M. Zeller, C.B. Nasr, Acta Cryst E66 (2010) m1145–m1146.
[39] T. Pivetta, F. Trudua, E. Valletta, F. Isaia, C. Castellano, F. Demartin, R. Tuveri, S. Vascellari, *A. pani*. J. Inorg. Biochem. 141 (2014) 103–113.
[40] X. Li, Z. Zhang, C. Wang, T. Zhang, K. He, F. Deng. J. Inorg. Biochem. 105 (2011) 23–30.
[41] G.A. Van Albada, I. Dominicus, I. Mutikainen, U. Turpeinen, J. Reedijk. Polyhedron 26 (2007) 3731–3736.
[42] M.C. Etter, J.C. MacDonald, J. Bernstein, Acta Cryst B46 (1990) 256–262.
[43] M. McCann, A.L.S. Santos, B.A. da Silva, M.T.V. Romanos, A.S. Pyrrho, M. Devereux, K. Kavanagh, I. Fichtner, A. Kellet, Toxicol. Res. 1 (2012) 47–54.
[44] C. Santini, M. Pellei, V. Gandin, M. Porchia, F. Tisato, C. Marzano, Chem. Rev. 114 (2014) 815–862.
[45] M. Bravo-Gomez, J.C. Garcia-Ramos, I. Gracia-Mora, L. Ruiz-Azuara, J. Inorg. Biochem. 103 (2009) 299–309.
[46] D. İnci, R. Aydın, Ö. Vatan, T. Sevgi, D. Yılmaz, Y. Zorlu, Y. Yerli, B. Çoşut, E. Demirkan, N. Çinkılıç, J. Biol. Inorg. Chem. 22 (2017) 61–85.
[47] A. Marín-Hernandez, I. Gracia-Mora, L. Ruiz-Ramírez, R. Moreno-Sanchez, Biochem. Pharmacol. 65 (2003) 1979–1989.
[48] R. Singh, R.N. Jadeja, M.C. Thounaojam, T. Patel, R.V. Devkar, D. Chakraborty, Inorg. Chem. Commun. 23 (2012) 78–84.
[49] S. Patitungkho, S. Adsule, P. Dandawate, S. Padhye, A. Ahmad, F.H. Sarkar, Bioorg. Med. Chem. Lett. 21 (2011) 1802–1806.
[50] K.M. Vyas, R.N. Jadeja, D. Patel, R.V. Devkar, V.K. Gupta, Polyhedron 80 (2014) 20–33.
[51] E.K. Efthimiadou, H. Thomadaki, Y. Sanakis, C.P. Raptopoulou, N. Katsaros, A. Scorilas, A. Karaliota, G. Psomas, J. Inorg. Biochem. 101 (2007) 64–73.
[52] C. Fernandes, A. Horn Jr., B.F. Lopes, E.S. Bull, N.F.B. Azeredo, M.M. Kanashiro, F.V. Borges, A.J. Bortoluzzi, B. Szpoganicz, A.B. Pires, R.W.A. Franco, J.C. de Almeida, L.L.F. Maciel, J.A.L.C. Resende, G. Schenk, J. Inorg. Biochem. 153 (2015) 68–87.
[53] K.G. Daniela, P. Gupta, R.H. Harbach, W.C. Guida, Q.P. Dou, Biochem. Pharmacol.

67 (2004) 1139–1151.
[54] Xue-Quan Zhou, Y. Li, Dong-Yan Zhang, Y. Nie, Zong-Jin Li, W. Gu, X. Liu, Jin-Lei Tian, Shi-Ping Yan, Eur. J. Med. Chem. 114 (2016) 244–256.
[55] Ferenc Zsila, Int. J. Biol. Macromol. 72 (2015) 1034–1040.
[56] M. Sinan, M. Panda, A. Ghosh, K. Dhara, P.E. Fanwick, D.J. Chattopadhyay, S. Goswami, J. Am. Chem. Soc. 130 (2008) 5185–5193.
[57] H.R. Dholariya, K.S. Patel, J.C. Patel, K.D. Pate, Spectrochim. Acta A Mol. Biomol. Spectrosc. 108 (2013) 319–328.
[58] A.E. Hoffman, M. DeStefano, C. Shoen, K. Gopinath, D.F. Warner, M. Cynamon, R.P. Doylea, Eur. J. Med. Chem. 70 (2013) 589–593.
[59] J.C. Almeida, I.M. Marzano, M. Pivatto, N.P. Lopes, A.M. Da Costa Ferreira, F.R. Pavan, I.C. Silva, E.C. Pereira-Maia, G. Von Poelhsitz, W. Guerra, Inorg. Chim. Acta 446 (2016) 87–92.
[60] F.R. Pavan, D.N. Sato, C. Q., F. Leite, An approach to the search for new drugs against tuberculosis, in: P.-J. Cardona (Ed.), Mycobacterium tuberculosis/book 2, Intech, 2011.